

Electronic Supplementary Information (ESI)

Nitrogen-doped Graphene-Vanadium Carbide Hybrids as High-performance Oxygen Reduction Reaction Electrocatalyst Support in Alkaline Media

Taizhong Huang^{1,2‡*}, Shun Mao^{1‡}, Haihui Pu¹, Zhenhai Wen¹, Xingkang Huang¹, Suqin Ci¹, and Junhong Chen^{1*}

¹Department of Mechanical Engineering, University of Wisconsin-Milwaukee, 3200 N Cramer Street, Milwaukee, WI 53211, USA.

²Key Laboratory of Chemical Sensing & Analysis in Universities of Shandong, School of Chemistry and Chemical Engineering, University of Jinan, Jinan, 250022, China

Experimental methods

Sample preparation: GO was produced from natural graphite powder using the modified Hummers method reported previously³⁷. The graphene-supported V₂O₃ was prepared by using a hydrothermal method with VCl₃ and GO as precursors. Then, 0.2 g VCl₃ (97%, Aldrich) and 8.0 ml GO (10 mg/ml in DI water) were mixed with ultrasonication for 30 minutes. The reaction was carried out at 200 °C for eight hours and the obtained precipitation was washed with a large amount of DI water and then dried at 100 °C for four hours. The resulting graphene-supported V₂O₃ was annealed at 1,000 °C in a hydrogen gas flow (0.5 lpm) for two hours to synthesize the VC nanocrystals. The nitrogen doping was accomplished by annealing the prepared samples at 1,000 °C under an ammonia atmosphere (0.5 lpm) for two hours. The loading of Pt nanocrystals on G-VC or N-G-VC was conducted by ultrasonic treatment of prepared materials in an H₂PtCl₆ solution. In a typical procedure, G-VC/N-G-VC and ethylene glycol (99%, Acros) were mixed with the H₂PtCl₆ solution (0.01 M, Alfa Aesar) and ultrasonicated for 30 minutes, from which Pt nanocrystals were produced and decorated on the surface of G-VC or N-G-VC. The Pt loading on the G-VC and N-G-VC was calculated as 10 wt.% based on the amount of H₂PtCl₆. The as-prepared Pt/N-G-VC sample was annealed at 200 °C for two hours under Ar atmosphere to improve the binding between N-G-VC and Pt nanocrystals as well as the crystallinity of Pt nanocrystals.

Characterization: The morphology of as-prepared samples, the selected area electron diffraction (SAED) pattern, the energy-dispersive X-ray spectroscopy (EDS), and the elemental mapping were obtained using a Hitachi (H 9000 NAR) transmission electron microscope (TEM) and a Hitachi (S-4800) scanning electron microscope (SEM) equipped with an energy-dispersive X-ray spectroscopy analyzer. Powder X-ray diffraction (XRD) was performed on a Scintag XDS 2000 X-ray powder diffractometer with monochromatized CuK α radiation ($\lambda=1.5418$ Å); the data were collected between scattering angles (2θ) of 10 and 80°. Based on the XRD results, the corresponding cell parameters of each sample were calculated using the Jade software. X-ray photoelectron spectroscopy (XPS) was conducted using an HP 5950A ESCA spectrometer with an MgK α source.

Electrochemical testing: The electrochemical characterization was carried out in 1 M KOH at room temperature using a CHI 600 electrochemical workstation with RRDE-3A electrode (CHI Inc., USA). The three-electrode cell consisted of an Ag/AgCl electrode as the reference electrode, Pt as the counter-electrode, and a glassy carbon electrode with various catalysts as the working electrode. To prepare the working electrode, 5.0 mg as-synthesized catalyst was mixed with 50 μ l Nafion solution (5.0 % Nafion in ethanol) and 450 μ l DI water. The mixture was sonicated and 5.0 μ l suspension was applied onto a glassy carbon electrode with a diameter of 3 mm and then fully dried. Before electrochemical tests, the working electrode was kept in an Ar-saturated electrolyte by cycling the potential from 0.2 to -0.8 V at a scan rate of 0.1 V·s⁻¹ until reproducible cyclic voltammograms were obtained. Thereafter, the electrolyte was saturated with oxygen and CVs were carried out and recorded for oxygen reduction from 0.2 to -0.8 V at a scanning rate of 0.005-0.1 V·s⁻¹. For comparison, the performance of commercial Pt/C catalyst (HP 10% Platinum on Vulcan XC-72 1g, Fuel Cell Store) was also tested under the same condition.

Modeling: Density functional theory (DFT) calculations were carried out using the full potential linearized augmented plane wave (FLAPW) method as implemented in *flair*.¹ The Generalized gradient approximation (GGA) in the formalism of Perdew, Burke, and Ernzerhof (PBE)² was adopted for the treatment of exchange-correlation. The cutoff energy of the plane wave basis was 12.25 Ry. The sphere radii were selected as 1.4 a_B for both C and N atoms and 2.4 a_B for V atom. The unit cell of VC was optimized with force within 0.001 eV/Å and the lattice constant was found to be 4.13 Å. The slab was modeled by 2×2×2 supercell with bulk cleaved (001) surface and the vacuum region was kept above 15 Å to minimize the interactions between adjacent slabs. 8×8×4 k-point mesh grids in the supercell were used for density of states calculation. *Ab-initio* Car-Parrinello molecular dynamics (CPMD) calculations were performed by taking advantage of the plane wave package under the Quantum Espresso distribution.³ A norm-conserving pseudopotential was adopted to treat the core electrons with energy (charge density) cutoff up to 80 Ry (320 Ry), while the exchange-correlation functional was the GGA in the formalism of PBE.² The simulation was performed in a canonical moles (N), volume and temperature (NVT) ensemble with the Nose Hoover thermostat for temperature 300 K at a time step of 0.024 fs. The ionic dynamics was simulated using the standard Verlet algorithm.

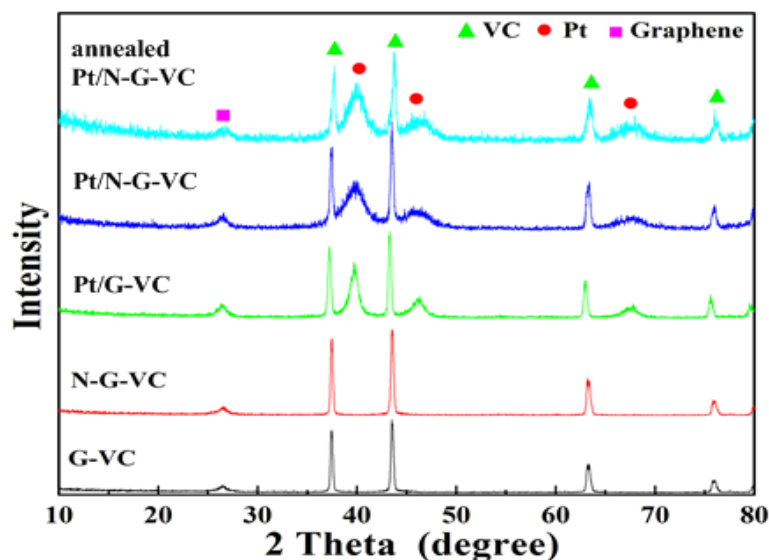


Figure S1. XRD results of G-VC, N-G-VC, Pt/G-VC, Pt/N-G-VC, and annealed Pt/N-G-VC.

The crystallographic structure of the as-prepared catalysts was investigated by XRD (Figure S1). The crystallinity of cubic VC (JCPDS No. 74-1220) is evidenced by diffraction peaks corresponding with (111), (200), (220), and (311) crystal facets. The graphene diffraction peak at 26.5° (200) is observed in all prepared samples, which indicates the GO was reduced to graphene in the catalyst synthesis process. The Pt nanocrystals with cubic structure (JCPDS No. 01-1194) are found in Pt-loaded catalysts with (111), (200), (220) crystal facets. Based on the XRD results, the VC phase is the main phase in catalysts and the doped nitrogen does not induce significant phase changes. The corresponding cell parameters are calculated for the prepared catalysts and results are shown in Table S1. There is a slight decrease in the crystal cell parameter of the VC with the doping of nitrogen, which is due to the difference between the atomic radius of nitrogen (0.075 nm) and carbon (0.091 nm).

Table S1. Phase and corresponding cell parameters of as-prepared catalysts (FCC refers to face-centered cubic).

Sample	Phase	Cell parameter
G-VC	VC (FCC)	$a = 0.4161$ nm
N-G-VC	VC (FCC)	$a = 0.4159$ nm
Pt/G-VC	VC (FCC)	$a = 0.4161$ nm
Pt/N-G-VC	Pt (FCC)	$a = 0.3937$ nm
	VC (FCC)	$a = 0.4159$ nm
Annealed Pt/N-G-VC	Pt (FCC)	$a = 0.3934$ nm
	VC (FCC)	$a = 0.4159$ nm
	Pt (FCC)	$a = 0.3932$ nm

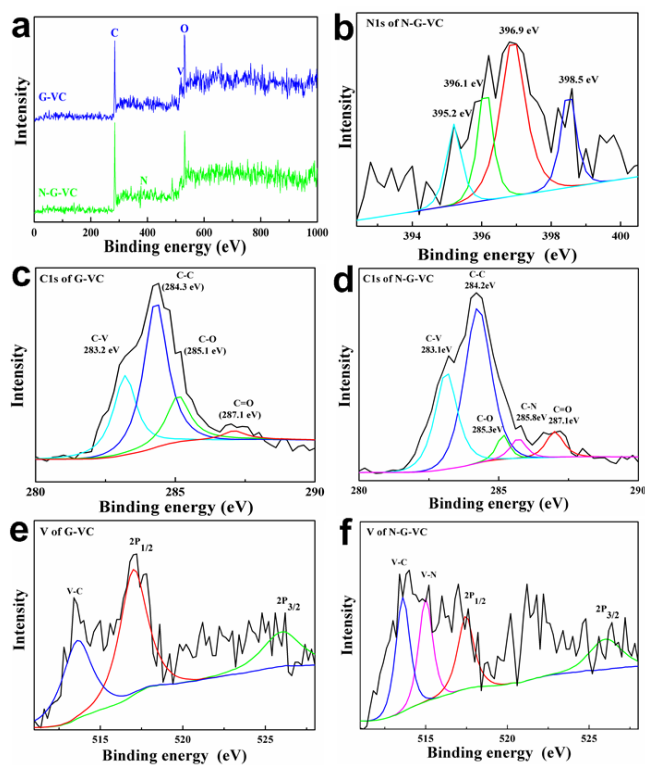


Figure S2. XPS survey spectrum (a) and curve fit of N1s spectra of N-G-VC (b), C1s spectra of G-VC (c) and N-G-VC (d), and V spectra of G-VC (e) and N-G-VC (f).

The surface chemical composition of the G-VC and N-G-VC was characterized by XPS analysis. Based on the survey spectra of G-VC and N-G-VC (Figure S2a), C1s, O1s, and V with different valence states are present, and N1s is present in the N-doped G-VC samples. Based on the high-resolution C1s spectrum (Figure S2c and d), four peaks centered at 283.2, 284.3, 285.1, and 287.1 eV are observed, corresponding with C-V, C-C, C-O, and C=O groups, respectively. Those groups indicate the presence of graphene and VC, as well as oxygen-containing groups in the graphene, *e.g.*, hydroxyl, epoxide, and carbonyl. As shown in Figure S2d, the C-N group (285.8 eV) is observed, which confirms the successful doping of nitrogen in graphene. The high-resolution N1s spectrum of N-G-VC can be fit into four peaks at 395.2, 396.1, 396.9, and 398.5 eV (Figure S2b). Those N1s peaks have a shift around 3.0 eV towards a lower binding energy compared with standard N1s.⁴ The peaks with a lower binding energy located at about 395.2 and 396.1 eV correspond with pyridine-like and pyrrole-like nitrogen, which can contribute to the π -conjugated system with a pair of p-electrons in the graphene layers. Nitrogen atoms within the graphene layers in the form of “graphitic” nitrogen lead to the XPS peak located at 396.9 eV, and the high-energy peak at 398.5 eV is commonly attributed to oxidized nitrogen. The V spectra in Figure S2e and f show two peaks corresponding with V2p_{1/2} and V2p_{3/2} and one peak relating to VC. In the N-G-VC sample, the V-N group (514.9 eV) is observed, indicating the nitrogen was also doped into the VC and occupied some crystal cell positions of carbon. The XPS results indicate the catalysts consist of VC nanocrystals and graphene with residue oxygen groups, and nitrogen is successfully doped into both graphene and VC after thermal annealing in ammonia.

The electron transfer number (*n*) calculation

The rotating disk electrode (RDE) measurement was carried out to study the kinetics of electrochemical catalytic ORR of the prepared catalyst. The polarization curves with different rotation rates (Figure 5a) and their corresponding Koutecky-Levich plots (Figure 5b) with the inverse current density (J^{-1}) versus the inverse of the square root of the rotation speed ($\omega^{-1/2}$) at different potentials are given. The slopes of their best linear fit lines were used to calculate the electron transfer number (*n*) based on the Koutecky-Levich equation:

$$\frac{1}{J} = \frac{1}{J_L} + \frac{1}{J_K} = \frac{1}{B\omega^{1/2}} + \frac{1}{J_K}$$

$$B = 0.62nFC_o(D_o)^{2/3}\nu^{-1/6}$$

$$J_K = nFkC_o$$

where *J* is the measured current density, J_K and J_L are the kinetic- and diffusion- limiting current densities, ω is the angular velocity, *n* is transferred electron number, *F* is the Faraday constant, C_o is the saturated concentration of O_2 in 1 M KOH at room temperature, D_o is diffusion coefficient of oxygen in water, ν is kinematic viscosity of the electrolyte at room temperature, and *k* is the electron-transfer rate constant. According to the Koutecky–Levich plot, the slope (1/*B*) can be used for calculating the electron transfer number, namely $n = B/(0.62FC_oD_o^{2/3}\nu^{-1/6})$.

Mass activity calculation

The mass activity of the catalyst samples was calculated from the reaction current of the catalyst at the $E_{1/2}$ point and the Pt amount in the hybrid catalyst using the following equation:

$$\text{Mass activity} = \frac{I}{m}$$

in which *I* is the reaction current of the catalyst at the $E_{1/2}$ and *m* is the Pt amount in the hybrid catalyst.

RHE conversion

A saturated silver chloride electrode was used as the reference electrode in all measurements. The measured potentials versus the Ag/AgCl reference electrode were converted to the reversible hydrogen electrode (RHE) scale via the Nernst equation:

$$E_{RHE} = E_{Ag/AgCl} + 0.059 \text{ pH} + E^o_{Ag/AgCl}$$

where E_{RHE} is the converted potential versus RHE, $E_{Ag/AgCl}$ is the experimental potential measured against the Ag/AgCl reference electrode, and $E^o_{Ag/AgCl}$ is the standard potential of Ag/AgCl at 25 °C (0.1976 V). The electrochemical measurements were carried out in 1 M KOH (pH = 14) at room temperature; therefore, $E_{RHE} = E_{Ag/AgCl} + 1.024$ V.

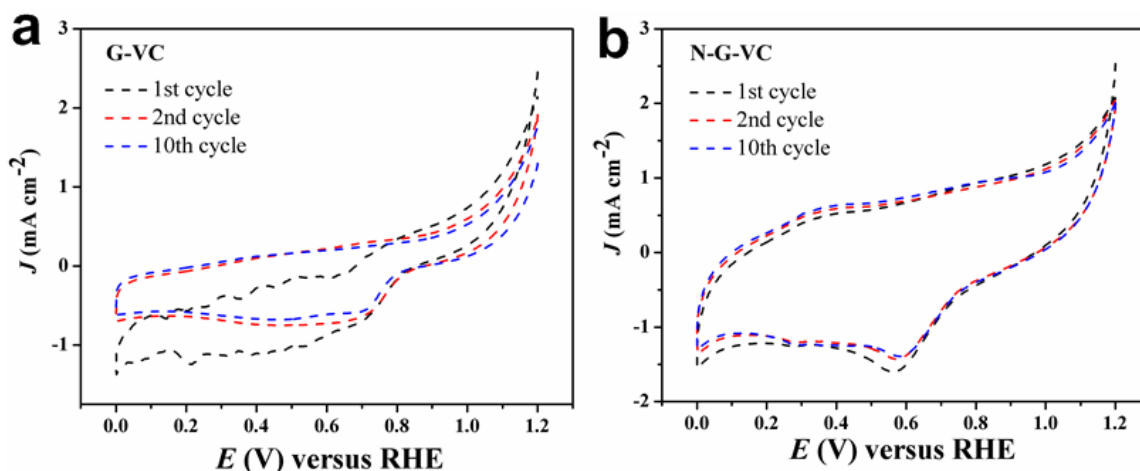


Figure S3. Cyclic voltammetry curves of (a) G-VC and (b) N-G-VC in O_2 -saturated 1 M KOH solution for the first, second, and tenth cycle at a scan rate of 0.05 V/s.

The catalysts were tested without pre-treatment by cyclic voltammetry under applied potentials comparable to those of a fuel cell (0 V - 1.2 V vs. RHE). The stability results show that the G-VC and N-G-VC are not electrochemically stable during the ORR, and significant drops in the reaction current are found from the first to the second cycle. However, after initial cycles the degradation in the catalyst activity is much smaller and the N-G-VC has a relatively smaller activity loss than the G-VC.

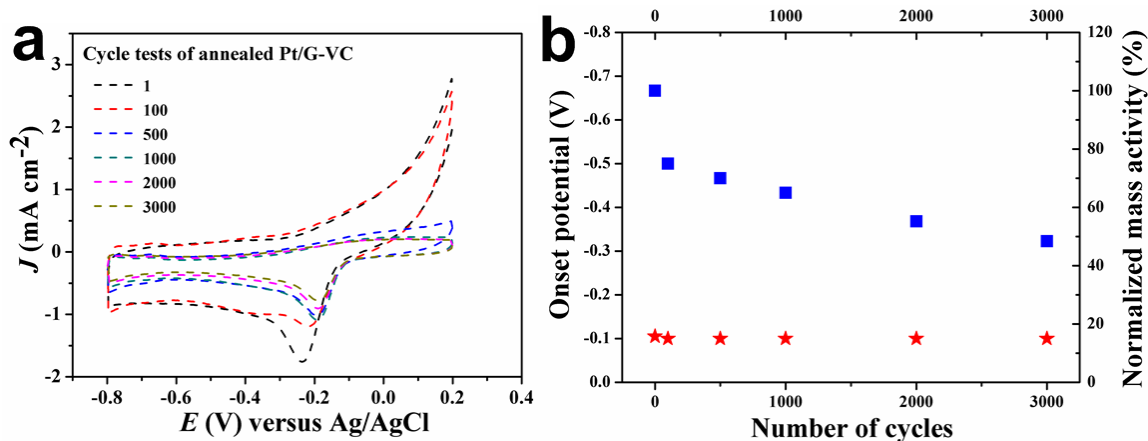


Figure S4. (a) Cyclic voltammetry curves of annealed Pt/G-VC in O_2 -saturated 1 M KOH solution for various potential cycles at a scan rate of 0.02 V/s. (b) Onset potential and normalized mass activity as a function of the number of cyclic voltammetry cycles for annealed Pt/G-VC.

Fig. S4a shows the CVs of annealed Pt/G-VC obtained after 1, 100, 500, 1,000, 2,000, and 3,000 cycles. The CVs indicate that the reaction current in the ORR gradually decreases. The onset potential and the calculated normalized mass activity (as a percentage of the initial mass activity in the first cycle at $E_{1/2}$) of the annealed Pt/G-VC as a function of the cycle number are shown in Fig. S4b. The onset potential of the catalyst has no obvious shift but the mass activity decreases to 65.0% and 48.4% after 1,000 and 3,000 cycles, respectively. Compared with Pt/N-G-VC (mass activity decreases to 82.2% and 72.4% after 1,000 and 3,000 cycles, respectively, Fig. 5f), the activity degradation in undoped Pt/G-VC is much larger, which suggests that nitrogen doping contributes to the enhanced stability of the electrocatalyst.

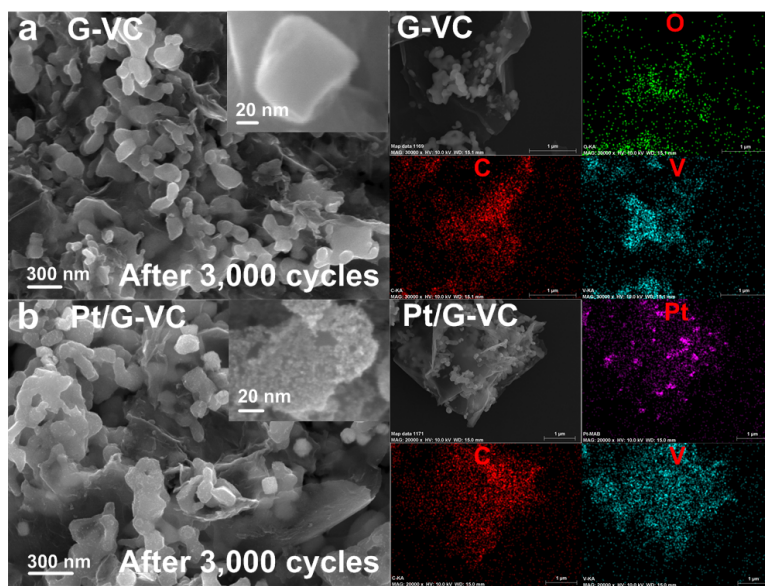


Figure S5. SEM images and elemental mapping of G-VC (a) and Pt/G-VC (b) catalysts after operating for 3,000 cycles.

Based on SEM images, the only change observed in the catalyst structure is slight agglomeration of the graphene and VC nanocrystals after the cycling test. Because VC nanocrystals are locally crystallized and grown on the surface of GO sheets, the binding between VC nanocrystals and GO is strong; therefore, the loss and agglomeration of VC nanocrystals during the cycling test is negligible. The element mapping of G-VC and Pt/G-VC after cycling tests further confirms that the hybrid structure was stable during the ORR and the hybrid catalyst structure was virtually unchanged after the cycling test, which leads to long-term stability of the catalysts. In addition, in our hybrid catalysts, there is no agglomeration or loss of Pt nanocrystals after cycling because the Pt nanocrystals are reduced in-situ and grown on the surface of the G-VC catalyst followed by annealing treatment under high temperature, leading to strong binding between Pt nanocrystals and graphene and VC. The negligible changes in our hybrid catalyst structure after cycling further explain the superior catalyst durability in ORR and indicate that the in-situ growth of Pt and thermal annealing could effectively improve the stability of the catalyst.